© 2019. Published by The Company of Biologists Ltd | Journal of Cell Science (2019) 132, jcs227389. doi:10.1242/jcs.227389

RESEARCH ARTICLE

STIM1-dependent membrane insertion of heteromeric TRPC1–TRPC4 channels in response to muscarinic receptor stimulation

Keita Harada, Hidetada Matsuoka and Masumi Inoue*

ABSTRACT

Muscarinic receptor stimulation results in activation of nonselective cation (NSC) channels in guinea pig adrenal medullary (AM) cells. The biophysical and pharmacological properties of the NSC channel suggest the involvement of heteromeric channels of TRPC1 with TRPC4 or TRPC5. This possibility was explored in PC12 cells and guinea pig AM cells. Proximity ligation assay (PLA) revealed that when exogenously expressed in PC12 cells, TRPC1 forms a heteromeric channel with TRPC4, but not with TRPC5, in a STIM1-dependent manner. The heteromeric TRPC1–TRPC4 channel was also observed in AM cells and trafficked to the cell periphery in response to muscarine stimulation. To explore whether heteromeric channels are inserted into the cell membrane, tags were attached to the extracellular domains of TRPC1 and TRPC4. PLA products developed between the tags in cells stimulated by muscarine, but not in resting cells, indicating that muscarinic stimulation results in the membrane insertion of channels. This membrane insertion required expression of full-length STIM1. We conclude that muscarinic receptor stimulation results in the insertion of heteromeric TRPC1–TRPC4 channels into the cell membrane in PC12 cells and guinea pig AM cells.

KEY WORDS: TRPC1, TRPC4, PC12 cell, Adrenal medullary cell, Muscarinic receptor, STIM1

INTRODUCTION

Acetylcholine released from the sympathetic preganglionic nerve fiber has been shown to mediate neuronal transmission through binding to the families of muscarinic acetylcholine receptors (mAChR) and nicotinic acetylcholine receptors (nAChR) in guinea pig adrenal medullary (AM) cells (Inoue et al., 2012). In addition, muscarinic receptor stimulation in AM cells of various mammals results in catecholamine secretion (Olivos and Artalejo, 2008; Inoue et al., 2018). The ionic mechanisms for muscarinic receptor-mediated excitation in AM cells differ among species of mammals, and their details have not yet been sufficiently elucidated (Inoue et al., 2018). In rat AM cells, muscarinic M_1 receptor (also known as Chrm1) stimulation (Harada et al., 2015) induces the endocytosis of TASK1 (also known as Kcnk3) channels with a consequent decrease in K^+ channel activity (Inoue et al., 2008; Matsuoka and Inoue, 2017; Inoue et al., 2019b), whereas in guinea pig AM cells the muscarinic receptor-mediated excitation is ascribed to not only TASK1 channel inhibition, but also to nonselective cation (NSC) channel activation (Inoue and Kuriyama, 1991; Inoue et al., 2012). This muscarinic receptor-regulated NSC channel has reversal potential of 0 mV and exhibits a conductance decrease at membrane potentials below −50 mV: i.e. the current–voltage (I–V) curve shows a negative slope at membrane potentials below −50 mV (Inoue and Kuriyama, 1991; Inoue et al., 2012). Moreover, La^{3+} has a double effect of facilitation and inhibition on the muscarinic NSC channel (Inoue et al., 2012). These properties of the NSC channel indicate the possible involvement of heteromeric channels of TRPC1 with TRPC4 or TRPC5 (Strübing et al., 2001; Clapham, 2003; Jung et al., 2003; Semtner et al., 2007). Indeed, the expression of TRPC1, TRPC4, and TRPC5 in guinea pig AM cells have been confirmed at the protein level: TRPC1 and TRPC4 are mainly located in the cytoplasm, whereas TRPC5 is present in the vicinity of, or at, the cell membrane.

The role of STIM1 in the regulation of TRPC channel activity has been disputed (Yuan et al., 2007; DeHaven et al., 2009). Thus, whether or not STIM1 plays an essential role in muscarinic receptor-regulated NSC channel activation in guinea pig AM cells needs to be investigated. STIM1 is expressed in guinea pig AM cells (Inoue et al., 2012), whereas it is present in rat adrenal cortical cells, but not AM cells (Matsuoka et al., 2009). What is interesting in rat AM cells is that although several forms of TRPC channels are present, as detected at the protein and/or mRNA levels, muscarinic receptor stimulation does not result in an apparent activation of NSC channels (Inoue et al., 2008; Matsuoka et al., 2009).

The findings that in guinea pig AM cells, TRPC1 and TRPC4 are localized inside the cells whereas TRPC5 is at the cell periphery, suggest that TRPC1 may form a heteromeric channel with TRPC4, but not TRPC5. If that is the case, muscarinic receptor-mediated excitation in guinea pig AM cells could be ascribed to insertion of heteromeric TRPC1–TRPC4 channels into the cell membrane. Indeed, several isoforms of TRPC channel proteins endogenously or exogenously expressed, such as TRPC3 (Goel et al., 2007), TRPC5 (Bezzerides et al., 2004) and TRPC6 (Cayouette et al., 2004), have been demonstrated to be inserted into the cell membrane in response to G protein-coupled receptor (GPCR) or receptor tyrosine kinase stimulation. The present study aimed initially to investigate whether the TRPC1 isoform forms a heteromeric channel with TRPC4 or TRPC5 in guinea pig AM cells and PC12 cells, a cell line derived from rat AM cells (Greene and Tischler, 1976). Once this proved to be the case, we next aimed to elucidate the role of STIM1 in the formation of these heteromeric channels. Finally, we used immunocytochemical and functional analyses to explore whether muscarinic receptor stimulation facilitates insertion of heteromeric channels into the cell membrane.

Department of Cell and Systems Physiology University of Occupational and Environmental Health School of Medicine, Kitakyushu 807-8555, Japan.

*Author for correspondence (minoue@med.uoeh-u.ac.jp)

M.I., 0000-0003-4180-5238

Received 31 October 2018; Accepted 15 April 2019

Journal of Cell Science (2019) 132, jcs227389. doi:10.1242/jcs.227389

RESULTS

Proximity ligation assay

Proximity ligation assay (PLA) was employed to elucidate whether TRPC1 and TRPC4 form a heteromeric channel in PC12 cells, an immortalized rat AM cell line (Greene and Tischler, 1976). This method depends on the specificity of antibodies used. Thus, to explore the specificities of anti-TRPC1 and anti-TRPC4 antibodies, TRPC1–GFP and TRPC4–GFP were exogenously expressed in PC12 cells with STIM1–myc, and PLA between TRPC1 and TRPC4 was carried out with a combination of either mouse anti-TRPC1 and rabbit anti-TRPC4 antibodies or rabbit anti-TRPC1 and mouse anti-TRPC4 antibodies. As shown in Fig. 1A, PLA products mainly developed in PC12 cells expressing exogenous proteins with either of the antibody combinations, indicating that these antibodies were selective and that exogenous TRPC1 and TRPC4 form a heteromeric channel. This notion was further examined with exogenous expression of TRPC1–GFP and untagged TRPC4, and a combination of rabbit anti-GFP and mouse anti-TRPC4 antibodies. PLA products again developed almost exclusively in PC12 cells expressing exogenous proteins (Fig. 1A). Next, whether TRPC1 selectively forms a complex with TRPC4 rather than with TRPC5 was examined in PC12 cells where untagged TRPC1 and STIM1–myc were expressed together with TRPC4–GFP or TRPC5–GFP, and PLA was carried out with a combination of mouse anti-TRPC1 and rabbit anti-GFP antibodies. As shown in Fig. 1B, TRPC4–GFP proteins were diffusely distributed in the cytoplasm, especially with high clustering near the nucleus, whereas TRPC5–GFP proteins were present both in the cytoplasm and at the cell periphery. Although part of TRPC5–GFP was diffusely present in the cytoplasm, PLA products conspicuously developed in cells expressing TRPC1 with TRPC4–GFP, but not with TRPC5–GFP (Fig. 1B,C). Lastly, heteromer formation was biochemically examined (Fig. 1D). TRPC1 was detected in immunoprecipitates obtained with anti-GFP antibody from lysates of PC12 cells expressing TRPC4–GFP, but not GFP alone.

To elucidate whether or not STIM1 is obligatory for G protein-coupled receptor-mediated activation of TRPC channels (Yuan et al., 2007; Dehaven et al., 2009), the extent of heteromer formation was compared between control and exogenous STIM1-expressing PC12 cells. As shown in Fig. 2A,B, the simultaneous expression of

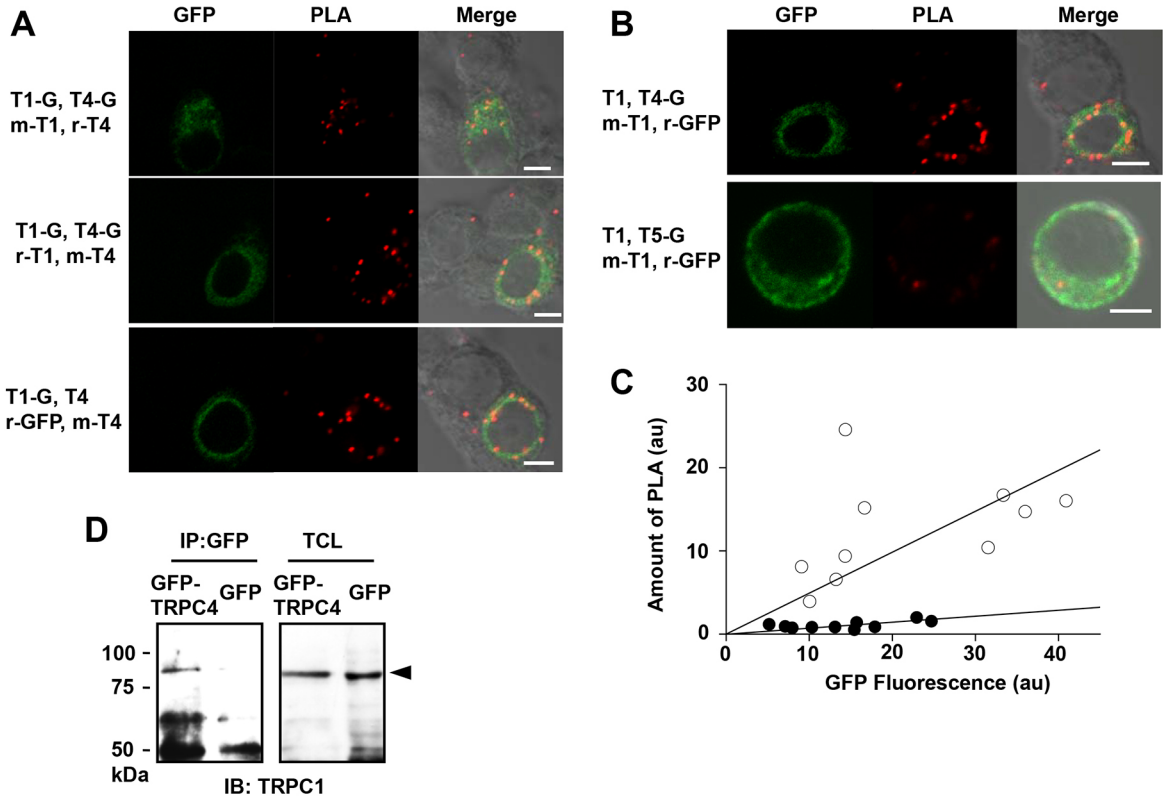

Fig. 1. Heteromeric channel formation of TRPC1 and TRPC4 in PC12 cells. (A) Proximity ligation assay (PLA) for heteromeric channel formation of TRPC1 and TRPC4 with a combination of mouse anti-TRPC1 (m-T1) and rabbit anti-TRPC4 (r-T4) antibodies, of rabbit anti-TRPC1 (r-T1) and mouse anti-TRPC4 (m-T4) antibodies, and of rabbit anti-GFP (r-GFP) and mouse anti-TRPC4 antibodies. PC12 cells were transfected to express TRPC1–GFP (T1-G) and TRPC4–GFP (T4-G) (first and second rows) or TRPC1–GFP and TRPC4 (third row), together with STIM1–myc. (B) Heteromeric channel formation of TRPC1 with TRPC4–GFP, but not with TRPC5–GFP (T5-G). PLA was performed with a combination of m-T1 and r-GFP antibodies. PC12 cells were transfected to express TRPC1 and TRPC4–GFP (first row) or TRPC5–GFP (second row), together with STIM1–myc. The left and middle columns represent confocal images of GFP and PLA fluorescence, respectively, and the right column shows a merge of differential interference contrast (DIC) and fluorescence images. GFP and PLA products were visible as FITC- and rhodamine-like fluorescence, respectively. (C) Levels of PLA products between TRPC1 and TRPC4–GFP (○) or TRPC5–GFP (●) are plotted against those of GFP fluorescence. Levels of fluorescence were expressed in arbitrary units (au). The data were approximated by $y=ax$ where y and x are levels of PLA products and GFP fluorescence, respectively, and a is the slope (0.4922 and 0.0719 for ○ and ●). The slope of 0.0719 significantly differs from 0 ($P<0.05$). (D) Immunoblot analysis of heteromeric channel formation of TRPC1 and TRPC4 in PC12 cells. Cell lysates were obtained from PC12 cells expressing TRPC4–GFP or GFP, and then subjected to immunoprecipitation with a mouse anti-GFP antibody (IP:GFP). The resulting immunoprecipitates were probed for TRPC1 with immunoblotting. The total cell lysates were also subjected to immunoblot (IB) analysis for TRPC1 (TCL). Scale bars: 5 µm.

Journal of Cell Science (2019) 132, jcs227389. doi:10.1242/jcs.227389

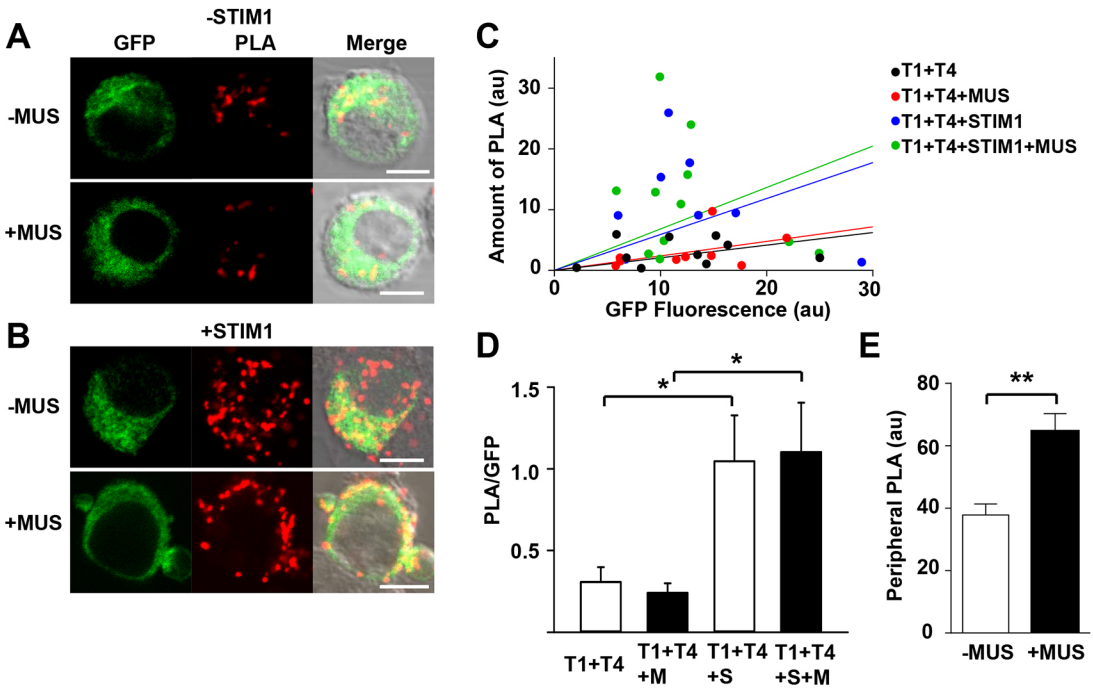

Fig. 2. Enhancement of heteromeric channel formation by exogenous expression of STIM1. (A,B) PLA for heteromeric channel formation of TRPC1–GFP (T1) and TRPC4–GFP (T4) in PC12 cells without (–STIM1) and with exogenous expression of STIM1–myc (+STIM1), respectively. PLA was performed with a combination of mouse anti-TRPC1 and rabbit anti-TRPC4 antibodies. The cells were not exposed (–MUS) or exposed to 30 µM muscarine for 2 min (+MUS). The left and middle columns represent confocal images of GFP and PLA fluorescence, respectively, and the right column is a merge of DIC and fluorescence images. (C) Levels of PLA fluorescence are plotted against those of GFP fluorescence. Levels of fluorescence were measured in arbitrary units (au). The slopes are 0.2079, 0.2386, 0.5919 and 0.6824 for T1+T4, T1+T4+MUS (M), T1+T4+STIM1 (S), and T1+T4+STIM1+MUS, respectively. (D) Summary of levels of PLA products in PC12 cells shown in C. The data represent means±s.e.m. of n=10 for T1+T4, n=9 for T1+T4+M, n=8 for T1+T4+S and n=11 for T1+T4+S+M. (E) Summary of fractions of PLA products located at the cell periphery out of the total in the whole-cell area. The cells were not stimulated (–MUS) or stimulated with 30 µM muscarine for 2 min (+MUS). The data represent means±s.e.m. of n=8 for –MUS and n=11 for +MUS. The open and closed columns represent non-stimulated and stimulated cells, respectively. *P<0.05, **P<0.01, evaluated by Mann–Whitney rank sum test. Scale bars: 5 µm.

STIM1–myc with TRPC1 and TRPC4 resulted in enhancement of PLA reactions between TRPC1 and TRPC4. Levels of rhodamine-like fluorescence (representing PLA products) were plotted against levels of FITC-like fluorescence (reflecting expression levels of TRPC1–GFP and TRPC4–GFP) (Fig. 2C). Levels of detected PLA products increased alongside levels of GFP fusion proteins, and the rate of increase in PLA products in cells expressing STIM–myc was significantly larger than in cells without it (Fig. 2D). In contrast to the previously reported effect on TRPC1–TRPC3 heteromer formation in HEK293 cells (Yuan et al., 2007), muscarinic stimulation did not affect the levels of PLA products between TRPC1 and TRPC4 (Fig. 2C,D). Intriguingly, some PLA products were translocated to the cell periphery in response to muscarinic stimulation (Fig. 2B,E).

STIM1 domains

STIM1 comprises several functional domains (Fig. 3A) (Lewis, 2011; Soboloff et al., 2012). Thus, we examined which domains were responsible for the facilitation of heteromer formation with the simultaneous expression of epitope-tagged STIM1 mutants and TRPC–GFP proteins. The STIM1ΔCt mutant contained STIM1 N-terminal residues 1–234, encompassing the transmembrane domain but not the CAD (CRAC activating domain), P/S (proline/serine-rich domain), TRIP (EBI binding sequence) or K (polybasic domain). The STIMCT (C-terminal) mutant contained residues 235–685 of STIM1, while the STIM1_1-448 mutant contained the N-terminus, transmembrane domain and CAD domain. PLA reactions between TRPC1 and TRPC4 scarcely occurred in PC12 cells expressing STIM1ΔCt, whereas the level of PLA products in cells expressing STM1_1-448 did not differ from that in cells expressing wild-type STIM1 (Fig. 3B,C). Intriguingly, expression of STIM1CT did not reproduce the PLA enhancement seen in cells expressing STIM1 or STM1_1-448. STIM1CT lacks the initial 234 amino acids of STIM1, corresponding to the intralumenal region and the transmembrane domain. Because of the deficit of this N-terminal region, STIM1CT exhibited a diffuse distribution in the cytoplasm, whereas wild-type STIM1 and the other two mutants were distributed in a reticular pattern suggesting their localization in the endoplasmic reticulum (ER). These results suggest that STIM1 (Lewis, 2011) helps TRPC1 and TRPC4 to form a heteromeric channel in the ER. This notion was further examined in cells where STIM1 was exogenously expressed with either TRPC1–GFP or TRPC4–GFP. As shown in Fig. 3D,E, PLA reactions between GFP and STIM1 occurred irrespective of whether cells expressed TRPC1–GFP (n=20) or TRPC4–GFP (n=16). These results suggest that there is a common sequence in TRPC1 and TRPC4 that binds to STIM1 in the ER (Huang et al., 2006).

TRPC1, TRPC4 and TRPC5 have been shown to bind to the STIM–Orai activating region (SOAR; amino acids 344–442) of STIM1, which almost coincides with the CAD region (amino acids 342-448). Thus, whether the CAD region is also involved in heteromeric TRPC1–TRPC4 channel formation was explored (Fig. 4A,B). When TRPC1–GFP and TRPC4–GFP were co-expressed with STIM1 CAD region construct CFP–CAD, the levels of PLA products for the

Journal of Cell Science (2019) 132, jcs227389. doi:10.1242/jcs.227389

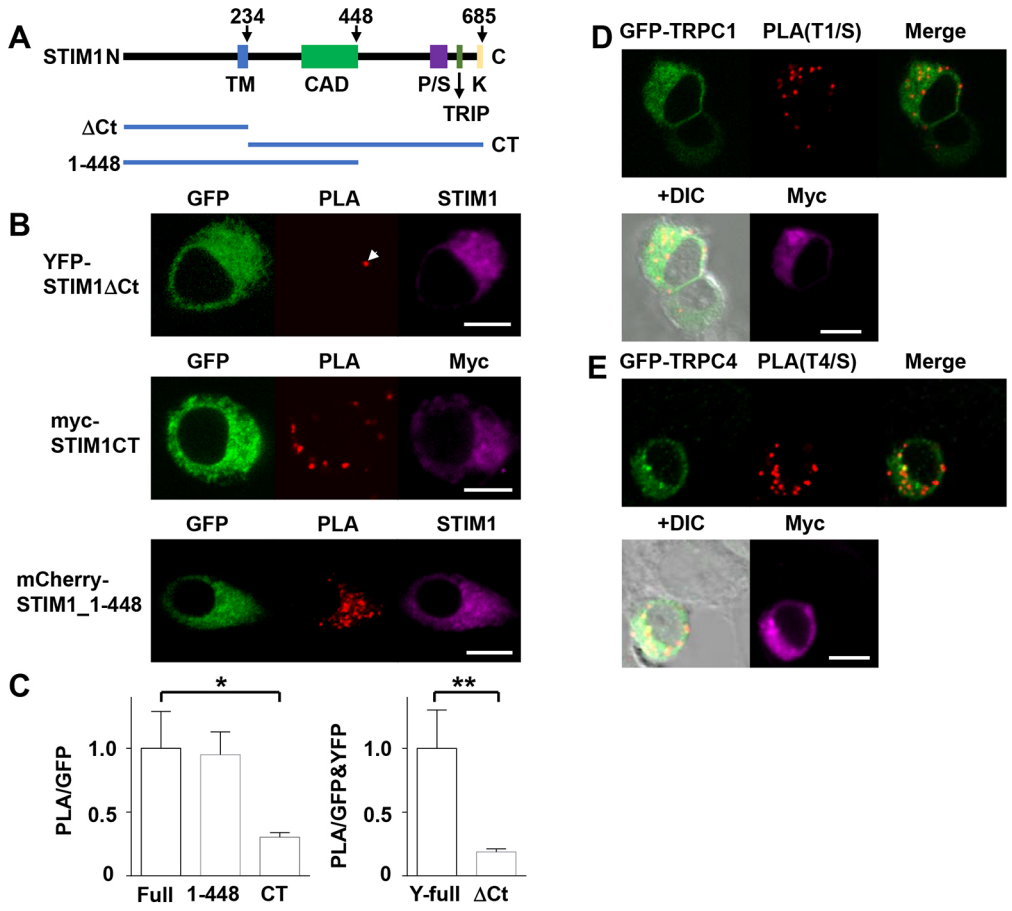

Fig. 3. STIM1 domains involved in heteromeric channel formation of TRPC1 and TRPC4. (A) Schematic of STIM1 structure comprising transmembrane (TM) domain, CRAC activating domain (CAD), proline/serine-rich domain (P/S), EBI binding sequence (TRIP) and polybasic domain (K), and configuration of STIM1 mutants. (B) PLA for heteromeric channel formation of TRPC1–TRPC4 in PC12 cells expressing TRPC1–GFP, TRPC4–GFP, together with one of the STIM1 mutants (YFP–STIM1ΔCt containing STIM1 amino acids 1–234; myc–STIM1CT, containing amino acids 235–685; mCherry–STIM1_1-448, containing amino acids 1–448). PLA was performed with a combination of rabbit anti-TRPC1 and mouse anti-TRPC4 antibodies. The left, middle and right columns represent confocal images of GFP, PLA and STIM1- or myc-like IR fluorescence, respectively. GFP, PLA reaction and STIM1- or myc-like IR material were visible as FITC-, rhodamine- and 633-like fluorescence, respectively. After the PLA reaction, the cells were treated with sheep anti-mouse IgG to mask mouse anti-TRPC1 antibody. Next, cells were treated with mouse anti-STIM1 or anti-myc antibodies, followed by treatment with goat anti-mouse IgG conjugated with Alexa Fluor 633. (C) Summary of relative levels of PLA products in PC12 cells expressing TRPC1–GFP, TRPC4–GFP, and one of the STIM1 mutants. Levels of PLA products between TRPC1–GFP and TRPC4–GFP were divided by those of GFP or the sum of GFP and YFP fluorescence. The values in cells expressing STIM1_1-448 (1-448) or STIM1CT (CT) were expressed as fractions of those in cells expressing full-length STIM1–myc (Full), whereas the value in cells expressing YFP–STIM1ΔCt (ΔCt) was expressed as a fraction of that in cells expressing full-length YFP–STIM1 (Y-full). Because the present setting to observe GFP cannot exclude YFP fluorescence, GFP fluorescence included YFP in PC12 cells expressing YFP–STIM1 full-length or mutant. Thus, the levels of PLA were divided by those of sum of GFP and YFP. The data represent means±s.e.m. of n=27 for Full, n=21 for 1-448, n=30 for CT, n=17 for Y-full and n=23 for ΔCt. *P<0.05, **P<0.01, evaluated by Tukey's multiple comparison test and by unpaired Student's t-test, respectively. (D,E) PLA for interaction between STIM1 and either TRPC1–GFP (D) or TRPC4–GFP (E). PC12 cells were transfected to express STIM1–myc and TRPC1–GFP or TRPC4–GFP. PLA between STIM1 and TRPC1–GFP (T1/S) or TRPC4–GFP (T4/S) was performed with a combination of mouse anti-STIM1 and either rabbit anti-TRPC1 or anti-TRPC4 antibodies, respectively. The top left and middle panels represent confocal images of GFP and PLA fluorescence, respectively; right panels are merge of first and second images; bottom left shows merge of DIC and third images; bottom right, confocal images of myc-like IR material. Scale bars: 5 µm.

heteromeric channel formation tended to decrease, but this decrease was not statistically significant. However, when heteromeric channel formation was augmented by the exogenous expression of STIM1–myc, the simultaneous expression of CFP–CAD resulted in a significant suppression of the heteromeric channel formation. These results support our notion that STIM1 facilitate heteromeric TRPC1–TRPC4 channel formation in the ER through its CAD region.

Insertion of TRPC channels into cell membrane

The translocation of TRPC1–TRPC4 channels to the cell periphery in response to muscarinic receptor stimulation raises the possibility that heteromeric channels are inserted into the cell membrane upon muscarine stimulation. This possibility was examined by transfecting PC12 cells with plasmids encoding mutated TRPC1–GFP and TRPC4–GFP proteins, in which FLAG and HA tags, respectively, were inserted into the extracellular domains of these channel proteins. The mutant proteins were expressed in PC12 cells with the same efficiency as the naïve TRPC–GFP proteins. Anti-HA and anti-FLAG antibodies were employed for PLA reactions to elucidate heteromeric channel formation and its membrane insertion. When PC12 cells expressing GFP proteins were not permeabilized (Fig. 5A,F), PLA products developed at the cell periphery in some of the stimulated cells, but never in the control cells. These findings were consistently observed in all the five trials where stimulated and non-stimulated cells were simultaneously

Journal of Cell Science (2019) 132, jcs227389. doi:10.1242/jcs.227389

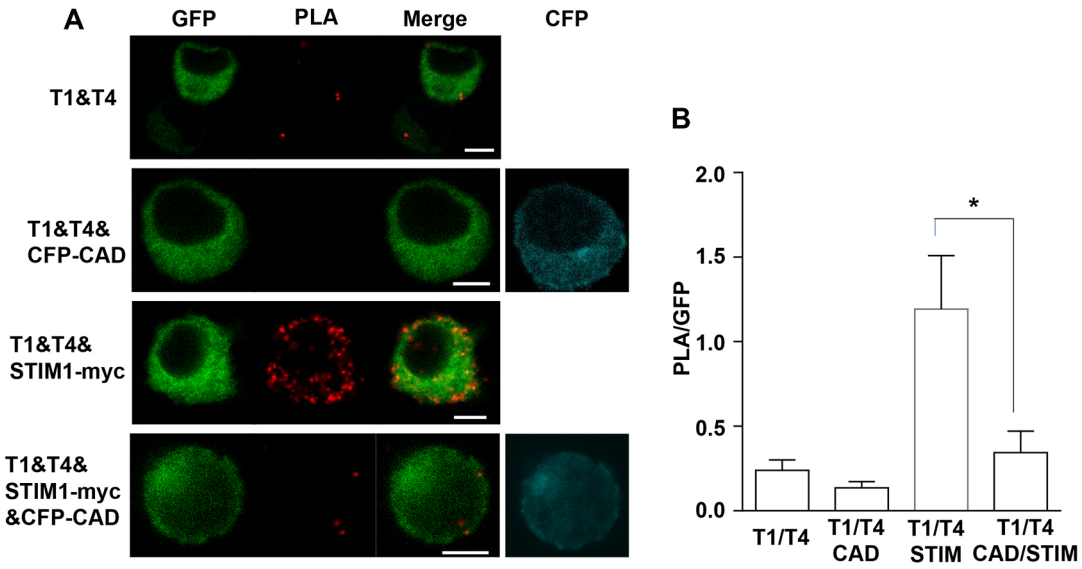

Fig. 4. Suppression of heteromeric TRPC1–TRPC4 channel formation by CAD. (A) PLA for heteromeric TRPC1–TRPC4 channel formation in PC12 cells exogenously expressing TRPC1–GFP and TRPC4–GFP (T1/T4) with or without CFP–CAD, STIM1–myc, or STIM1–myc and CFP–CAD. PLA was performed with a combination of mouse anti-TRPC1 and rabbit anti-TRPC4 antibodies. GFP, PLA products and CFP were visible as FITC-, rhodamine- and CFP-like fluorescence, respectively. Left, middle and far right columns represent FITC-, rhodamine- and CFP-like fluorescence, respectively, and right column is a merge of left and middle images. (B) Summary of PLA product levels in PC12 cells expressing T1/T4, T1/T4/CAD, T1/T4/STIM1 and T1/T4/STIM1/CAD. The level of PLA products was expressed as the ratio of the level of PLA fluorescence to that of GFP fluorescence in each cell. The data represent means±s.e.m. of n=15 for T1/T4, n=11 for T1/T4/CAD, n=9 for T1/T4/STIM1 and n=5 for T1/T4/STIM1/CAD. *P<0.05, evaluated by Tukey's multiple comparison test. Scale bars: 5 µm.

examined each time (sign test, P<0.05). In 74 stimulated cells, 59.5% exhibited PLA products at the cell periphery, whereas none of the 49 non-stimulated cells did. In contrast to non-permeabilized cells, similar levels of PLA products were observed in permeabilized stimulated (n=6) and non-stimulated cells (n=22; Fig. 5B). It is worth noting that at least some of the PLA products formed between the two different tags were trafficked to the cell periphery in response to muscarine stimulation (Fig. 5B).

Whether STIM1 is also involved in muscarine-induced trafficking of the heteromeric channel to the cell membrane was next explored in PC12 cells expressing mutated TRPC1–GFP and TRPC4–GFP proteins. As shown in Fig. 5D,F, PLA products between FLAG- and HA-tagged TRPC proteins did not develop at the cell periphery in response to muscarine stimulation in cells expressing STM1_1-448 (n=10). This STIM1 mutant does not contain several domains that are important for STIM1 to interact with membrane lipids (Lewis, 2011) or the cytoskeleton (Grigoriev et al., 2008). The result suggests that TRPC1–TRPC4 heteromeric channels are trafficked to the cell membrane through the C-terminus of STIM1.

Muscarinic receptor stimulation in PC12 cells is expected to produce an increase in intracellular calcium levels ($[Ca^{2+}]_i$) through mobilizing Ca^{2+} from Ca^{2+} store sites (Kim and Saffen, 2005; Ebihara et al., 2006). This Ca^{2+} mobilization might result in activation of store-operated Ca^{2+} entry (SOCE). Whether this process might be involved in membrane insertion of TRPC1–TRPC4 channels was investigated with the expression of a STIM1D76A mutant, which mimics Ca^{2+} depletion in Ca^{2+} store sites (Liou et al., 2005). As expected, the simultaneous expression of the STIM1 mutant with the HA- and FLAG-tagged TRPC channels in unstimulated cells resulted in translocation of PLA products to the cell periphery (n=8; Fig. 5E); however, it did not lead to insertion of the channels (n=54; Fig. 5C). Interestingly, muscarine-induced insertion of channels was significantly facilitated in cells expressing STIM1D76A: 89.5% of GFP-positive cells (n=38) exhibited a PLA reaction at the cell surface and the mean±s.e.m. of PLA products in such cells was also increased to 1.18±0.12, compared to 0.85±0.10 in wild-type STIM1-expressing cells (Fig. 5F).

Insertion of the STIM1 and TRPC4 complex into the cell membrane

The findings that STIM1 forms a complex with TRPC1 and TRPC4 raise the possibility that STIM1 is also trafficked to the cell membrane with the TRPC1–TRPC4 heteromeric channel. This possibility was examined with a combination of anti-STIM1 and anti-HA antibodies. If the complex of STIM1 and TRPC4–HA–GFP is inserted into the cell membrane, the extracellular domains of TRPC4 and the intralumenal domain of STIM1, where an epitope for the antibody is located, should be exposed to the extracellular space. We found that PLA products between STIM1 and TRPC4–HA–GFP developed exclusively in PC12 cells stimulated by muscarine but not under basal conditions (Fig. 5G,H).

Functional analysis of membrane insertion

The trafficking of TRPC1–TRPC4 heteromeric channels to the cell membrane in response to muscarine stimulation was functionally examined with a Ca^{2+} indicator. After PC12 cells were transfected with plasmids encoding TRPC1–GFP, TRPC4–GFP and STIM1–myc, they were loaded with Fura-2 to measure changes in $[Ca^{2+}]_i$. As shown in Fig. 6A,B, the increase in peak amplitudes of Ca^{2+} induced by treatment with 30 µM muscarine in PC12 cells expressing exogenous STIM1 and TRPC–GFP proteins did not differ from that in control cells, whereas sustained Ca^{2+} levels in the former were significantly larger than those in the latter (Fig. 6A,C). In addition, the resting Fura-2 ratio was 0.963±0.021 (n=15) in cells expressing TRPC–GFP proteins and STIM1, which did not differ significantly from 0.899±0.024 (n=17) in control cells. These results suggest that exogenously expressed TRPC1–TRPC4 channels have no channel activity in resting conditions and become active upon muscarinic receptor stimulation. This notion

Journal of Cell Science (2019) 132, jcs227389. doi:10.1242/jcs.227389

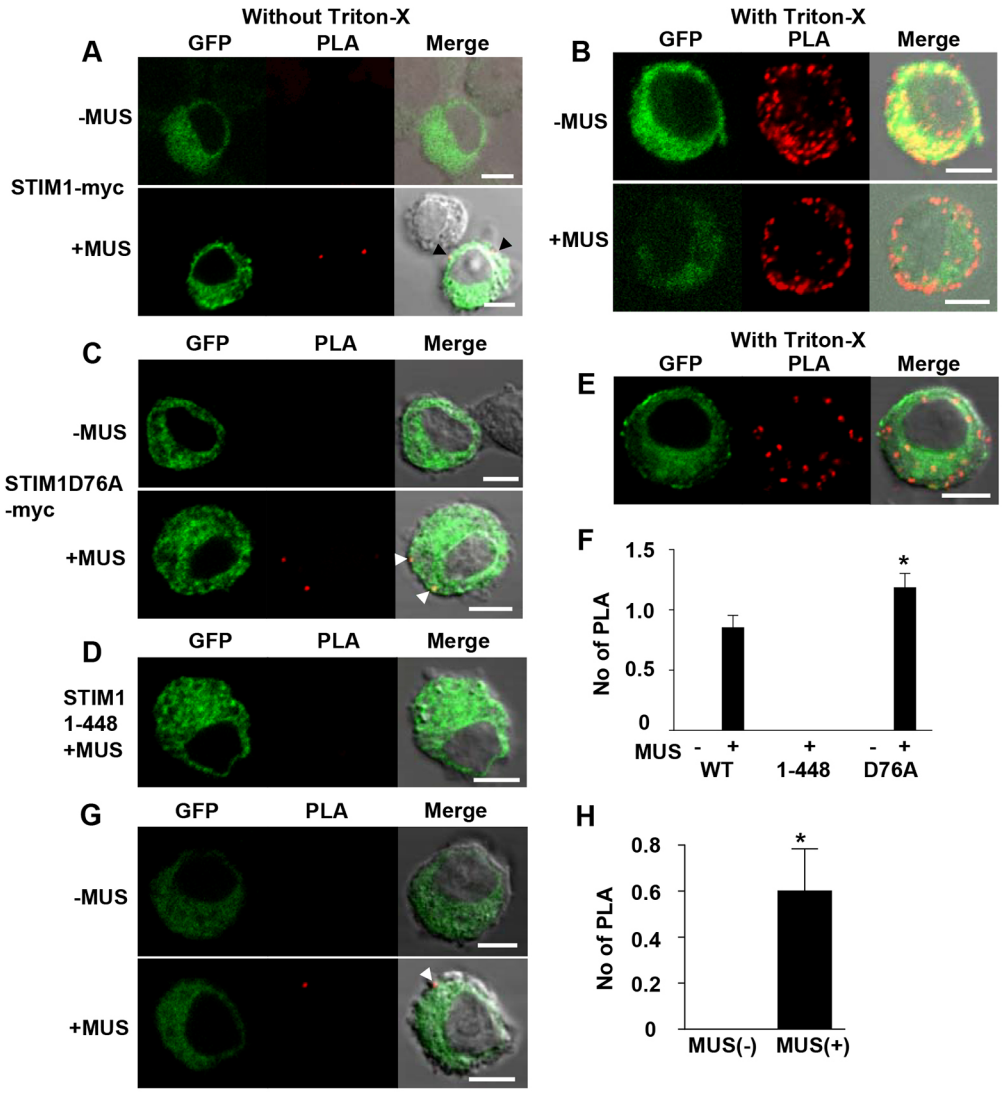

Fig. 5. Insertion of heteromeric TRPC1–TRPC4 channels and the complex of TRPC4 and STIM1 into the plasma membrane in response to muscarine stimulation, and role of STIM1 domains. (A,C,D) PLA for heteromeric TRPC1–TRPC4 channel formation in PC12 cells expressing STIM1–myc (A), STIM1D76A–myc (C), and STIM1_1-448 (D). PC12 cells were transfected to express TRPC1–GFP and TRPC4–GFP and full-length or mutant STIM1 as indicated. PC12 cells were unstimulated (−MUS) or stimulated with 30 µM muscarine for 30 s (+MUS), and then fixed with PFA. The cells were not permeabilized. (B,E) PLA for heteromeric TRPC1–TRPC4 channel formation in PC12 cells expressing STIM1–myc (B) and STIM1D76A–myc (E). Next, cells were unstimulated (−MUS) or stimulated with 30 µM muscarine for 30 s (+MUS), then permeabilized with 0.3% Triton X-100. (F) Summary of numbers (No) of PLA products between TRPC1–GFP and TRPC4–GFP in PC12 cells expressing full-length STIM1–myc (WT), STIM1_1-448 (1-448) or STIM1D76A–myc (D76A). The cells were unstimulated (−) or stimulated with 30 µM muscarine for 30 s (+), and then fixed with PFA and not permeabilized. GFP-positive cells were examined, and the numbers of PLA products in PLA-positive cells were averaged. The data represent means±s.e.m. of n=104 for WT–, n=74 for WT+, n=21 for 1-448+, n=54 for D76A–, n=38 for D76A+. *P<0.05, evaluated by unpaired Student's t-test. (G) PLA for interaction between TRPC4–GFP and STIM1 in PC12 cells unstimulated (−MUS) or stimulated with 30 µM muscarine for 30 s (+MUS). PC12 cells were transfected to express TRPC1–GFP, TRPC4–GFP and STIM1–myc. After stimulation, PC12 cells were fixed with PFA and not permeabilized. (H) Summary of numbers of PLA products between TRPC4–GFP and STIM1 in PC12 cells unstimulated (−MUS) or stimulated with muscarine for 30 s (+MUS). GFP-positive cells were examined, and the numbers of PLA products in PLA-positive cells were averaged. The data represent means±s.e.m. of n=10 for MUS(−) and n=20 for MUS(+). *P<0.05, evaluated by unpaired Student's t-test. In all PLA images, the left and middle columns represent confocal images of GFP and PLA, respectively, and the right column is a merge of DIC and fluorescence images. Scale bars: 5 µm.

was further explored with ML204, which is a specific inhibitor of TRPC4 and has no action on voltage-dependent Ca^{2+} channels (Miller et al., 2011). We have previously reported that in guinea pig AM cells muscarine failed to activate NSC channels in the presence of 10 µM ML204 (Inoue et al., 2019a). The sustained levels of muscarine-induced Ca^{2+} increases were significantly suppressed by the simultaneous application of ML204 with muscarine in PC12 cells expressing TRPC1–GFP and TRPC4–GFP (Fig. 6A,C).

Analyses in guinea pig AM cells

Our previous immunocytochemical studies have revealed that TRPC1- and TRPC4-like immunoreactive (IR) material is mainly present in the cytoplasm in guinea pig AM cells (Inoue et al., 2012). If TRPC1–TRPC4 heteromeric channels are involved in NSC currents activated by muscarinic agonists, they should be trafficked to the cell membrane in response to muscarine stimulation. Thus, this notion was immunocytochemically examined. As shown in Fig. 7A, TRPC1- and TRPC4-like IR material present in the

Journal of Cell Science (2019) 132, jcs227389. doi:10.1242/jcs.227389

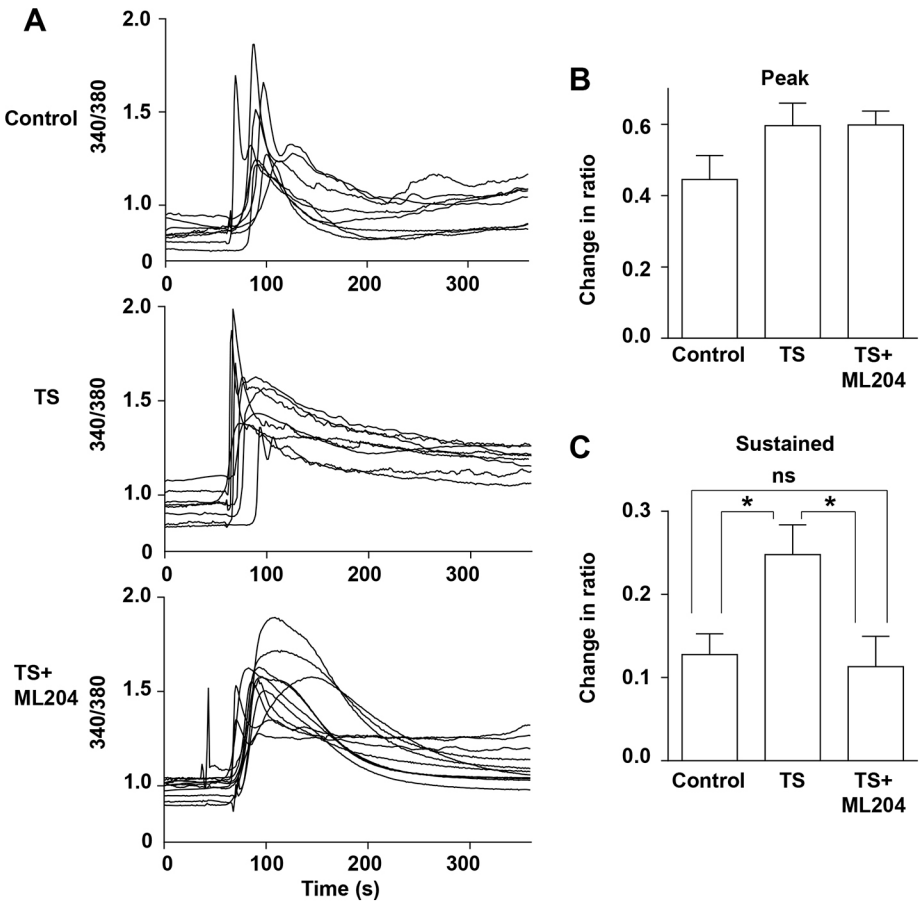

Fig. 6. Enhancement of muscarine-induced Ca^{2+} response by expression of TRPC1–GFP and TRPC4–GFP. (A) Muscarine-induced changes in Fura-2 ratio in PC12 cells with (TS) and without (Control) exogenous expression of TRPC1–GFP, TRPC4–GFP and STIM1–myc. GFP-positive cells were considered to be cells expressing the three exogenous proteins. 300 µM muscarine-containing standard saline solution (0.1 ml) with (TS+ML204) or without 100 µM ML204 (Control or TS) was added by a pipette to a dish solution (0.9 ml) (final concentrations of muscarine and ML204, 30 µM and 10 µM, respectively) ∼1 min after the start of measurement. Fura-2 ratio represents emission evoked at 340 nm divided by that at 380 nm (340/380), and was measured every 900 ms for 360 s (see Materials and Methods). (B,C) Muscarine-induced changes in Fura-2 ratio at peak (B) and sustained levels (C). The changes represent differences between the values before stimulation and those at the peak and sustained level after stimulation. The peak and sustained current levels represent averages of peak and last five points, respectively. The data represent means±s.e.m. of n=17 for control, n=15 for TS and n=11 for +ML204. *P<0.05; ns, not significant; evaluated by Tukey's multiple comparison test.

cytoplasm was trafficked to the cell periphery upon muscarine stimulation and co-localized with Na^+/K^+-ATPase α1 subunit (α1, also known as ATP1A1)-like IR material as a marker of the cell membrane. The level of α1-like IR material co-localized with TRPC1-like IR material (as a percentage of total TRPC1-like IR material) increased from 18.3% to 42.3%, whereas that of α1-like IR material co-localized with TRPC4-like IR material (as a percentage of the total TRPC4-like IR material) also increased from 24.0% to 37.7% (Fig. 7B). Furthermore, TRPC1-like IR material was coincident with TRPC4-like IR material (Fig. 7C), with TRPC1/TRPC4 and TRPC4/TRPC1 coincidence rates of 42.2% and 45.1%, respectively, and the values were not affected by muscarine stimulation (Fig. 7D). The coincidence of TRPC1-like and TRPC4-like IR material suggests that TRPC1 and TRPC4 form a heteromeric channel in guinea pig AM cells.

As discussed above, experiments in PC12 cells demonstrated that the anti-TRPC1 and anti-TRPC4 antibodies used were specific and useful for PLA. Thus, these reagents were employed to investigate directly whether TRPC1 forms a heteromeric channel with TRPC4 in guinea pig AM cells. As shown in Fig. 8A,B, PLA revealed that TRPC1 and TRPC4 form a heteromer, and that some of the heteromers were apparently trafficked to the cell membrane in response to stimulation with 30 µM muscarine. While TRPC5-like IR material has previously been detected at the cell periphery (Inoue et al., 2012), PLA reaction between TRPC5 and TRPC1 was scarcely found to occur (Fig. 8B,C).

Finally, an electrophysiological approach was used to examine whether TRPC4 or TRPC5 is inserted into the cell membrane in response to muscarine stimulation in guinea pig AM cells. One of the properties of TRPC4 and TRPC5 is that lantanides, such as La^{3+}, have a double action on channel activity, i.e. enhancement and suppression (Jung et al., 2003; Semtner et al., 2007). Thus, if the channels are located at the cell membrane, La^{3+} application is expected to induce an inward current at negative membrane potentials (Bezzerides et al., 2004). As shown in Fig. 8D, exposure to 600 µM La^{3+} resulted in development of an inward current at −60 mV in 64% of AM cells (n=11), a current which was sustained during La^{3+} treatment. By contrast, inward currents induced by 10 µM muscarine were transiently enhanced in the presence of La^{3+}. The peak amplitude of current evoked by the first application of muscarine in the presence of La^{3+} was 286.0±67.4% (n=6) of that in its absence. The extent of this enhancement was successively diminished upon repeated application of muscarine (Inoue et al., 2012), and the level of inward current at the end (40–50 s) of a third application in the presence of La^{3+} was 30.0±8.9% (n=6) of that in its absence. What is more noteworthy is that a noise level was markedly diminished during the development of inward currents, whereas the muscarine-induced currents were associated with an increase in current noise. To explore the ionic mechanism for La^{3+}-induced inward currents, I–V curves were examined with 50 ms pulses before and during La^{3+} application (Fig. 8E). The I–V curve for La^{3+}-induced current (Fig. 8F) showed that the current had an inwardly rectifying property with a reversal potential of −81.5±1.2 mV (n=4), a value which is close to the equilibrium potential for K^+ (−83.6 mV), suggesting that the current is at least in part due to inwardly rectifying K^+ channel inhibition (Inoue and Imanaga, 1993) and not to NSC channel activation. Taken together with the immunocytochemical findings, the electrophysiological results strongly suggest that muscarinic receptor stimulation in guinea pig AM cells results in

Journal of Cell Science (2019) 132, jcs227389. doi:10.1242/jcs.227389

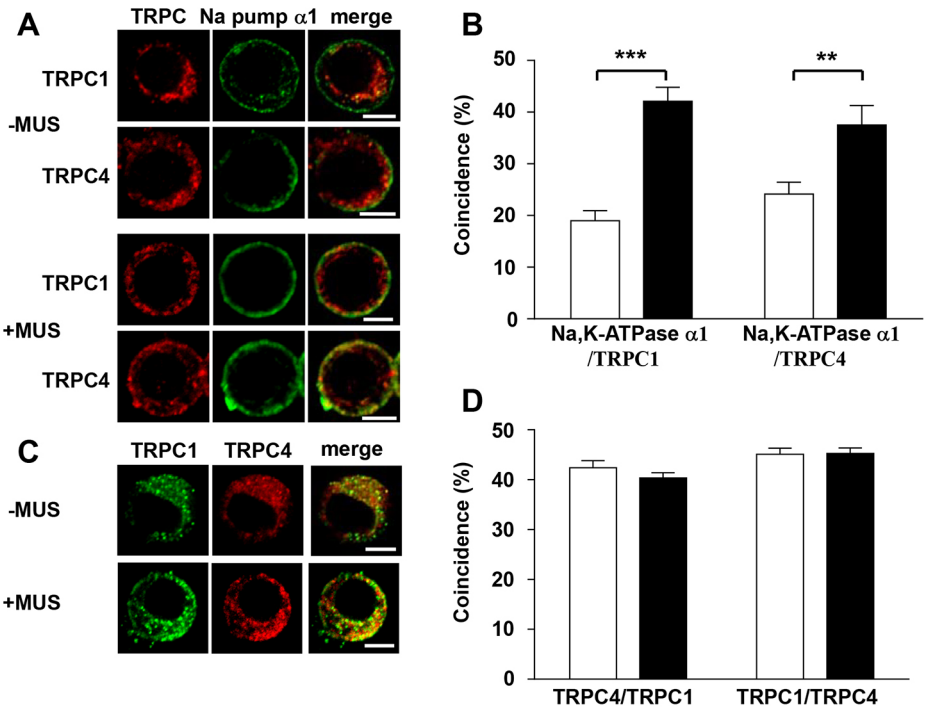

Fig. 7. Translocation of TRPC1 and TRPC4 to the plasma membrane in guinea pig AM cells in response to muscarine stimulation. (A) Confocal images of Na pump α1- and TRPC1- or TRPC4-like immunoreactive (IR) material in resting (–MUS) and stimulated (+MUS) adrenal medullary (AM) cells. Isolated AM cells were unstimulated or stimulated for 1 min by 30 µM muscarine and then fixed for 5 min with methanol at –20°C. After fixation, the cells were simultaneously treated with mouse anti-α1 and rabbit anti-TRPC1 or anti-TRPC4 antibodies overnight. α1- and TRPC1- or TRPC4-like IR material were observed as FITC- and rhodamine-like fluorescence, respectively. Left and middle columns represent confocal images of TRPC1- or TRPC4-like IR material and α1-like IR material, respectively, and the right column is a merge of left and middle columns. Co-localization of TRPC1- or TRPC4-like IR material with α1-like IR is shown in yellow. (B) Summary of percentages of TRPC1- or TRPC4-like IR material co-localized with α1-like IR material in resting and stimulated AM cells. The data represent means±s.e.m. of n=9 for TRPC1 –MUS (open), n=13 for TRPC1 +MUS (closed); n=8 for TRPC4 –MUS and n=8 for TRPC4 +MUS. **P<0.01, ***P<0.001, evaluated unpaired Student's t-test. (C) Co-localization of TRPC4-like IR material with TRPC1-like IR material and vice versa. After no stimulation (–MUS) or stimulation with 30 µM muscarine for 2 min (+MUS), guinea pig AM cells were fixed with PFA and then treated with mouse anti-TRPC1 and rabbit anti-TRPC4 antibodies. Red and green represent rhodamine- and FITC-like fluorescence, respectively, and yellow indicates coincidence of both fluorescence. (D) Summary of the extents of co-localization of TRPC1-like IR material with TRPC4-like IR material and vice versa. The data present means±s.e.m. of n=55 for –MUS (open) and n=109 for +MUS (closed). Scale bars: 5 µm.

the insertion of heteromeric TRPC1–TRPC4 channels into the cell membrane.

DISCUSSION

Activation mechanism

The TRPC family comprises seven isoforms, which are divided into three subgroups (Clapham, 2003): subgroup one comprises TRPC1, TRPC4 and TRPC5; subgroup two consists of TRPC3, TRPC6 and TRPC7; while TRPC2, which is a pseudogene in humans, forms subgroup three. Although stimulation of receptors coupled with Pertussis toxin-insensitive G proteins is known to activate a heteromer of TRPC1 and TRPC4 or TRPC5 (Strübing et al., 2001; Kim et al., 2014), the signal transduction mechanism is not yet sufficiently elucidated. In the present study, TRPC1 was found to conspicuously form a complex with TRPC4, but not TRPC5, in PC12 cells and guinea pig AM cells, and this heteromer was present in the cytoplasm under resting conditions and trafficked to the cell periphery in response to muscarine stimulations. In contrast to PC12 cells, TRPC4–GFP channels expressed in HEK293 cells have previously been shown to be located at the cell periphery (Schaefer et al., 2000), and TRPC4 proteins in HEK293 cells were surface labeled (Kim et al., 2014). These findings indicate that at least some TRPC4 proteins exogenously expressed in HEK293 cells are located at the cell membrane. Thus, interesting cell type-specific trafficking patterns exist. While TRPC4 and TRPC5 both were localized at the cell periphery in HEK293 cells, in PC12 cells (present results) and guinea pig AM cells (Inoue et al., 2012) TRPC4 was mainly present in the cytoplasm and TRPC5 at the cell periphery. Thus, AM cells and PC12 cells might lack the constitutively active machinery to transport TRPC4 proteins to the cell membrane. Alternatively, because TRPC1 and TRPC4 form a heteromeric channel in PC12 cells in a STIM1-dependent manner, TRPC1 or STIM1, resident proteins of the ER membrane (Lewis, 2011), might hinder the transport of TRPC4 to the cell membrane. As the expression level of STIM1 in HEK293 cells increases, the amount of TRPC5 immunoprecipitated together with TRPC1 has been shown to decrease (Alicia et al., 2008). This result raises the possibility that STIM1 hinders the heteromer formation of TRPC1 with TRPC5, possibly in the ER. Otherwise, TRPC1 would be trafficked to the cell membrane as a component of the heteromeric channel (Alfonso et al., 2008). Because PLA products between STIM1 and TRPC1 or TRPC4 developed in PC12 cells, it would be reasonable to conclude that TRPC1–TRPC4 heteromeric channels in PC12 cells and guinea pig AM cells are mainly present in the ER, along with STIM1.

The findings that mAChR stimulation in PC12 cells induced the trafficking of TRPC1–TRPC4 heteromeric channels to the cell membrane and an increase in $[Ca^{2+}]_i$ suggest that membrane

Journal of Cell Science (2019) 132, jcs227389. doi:10.1242/jcs.227389

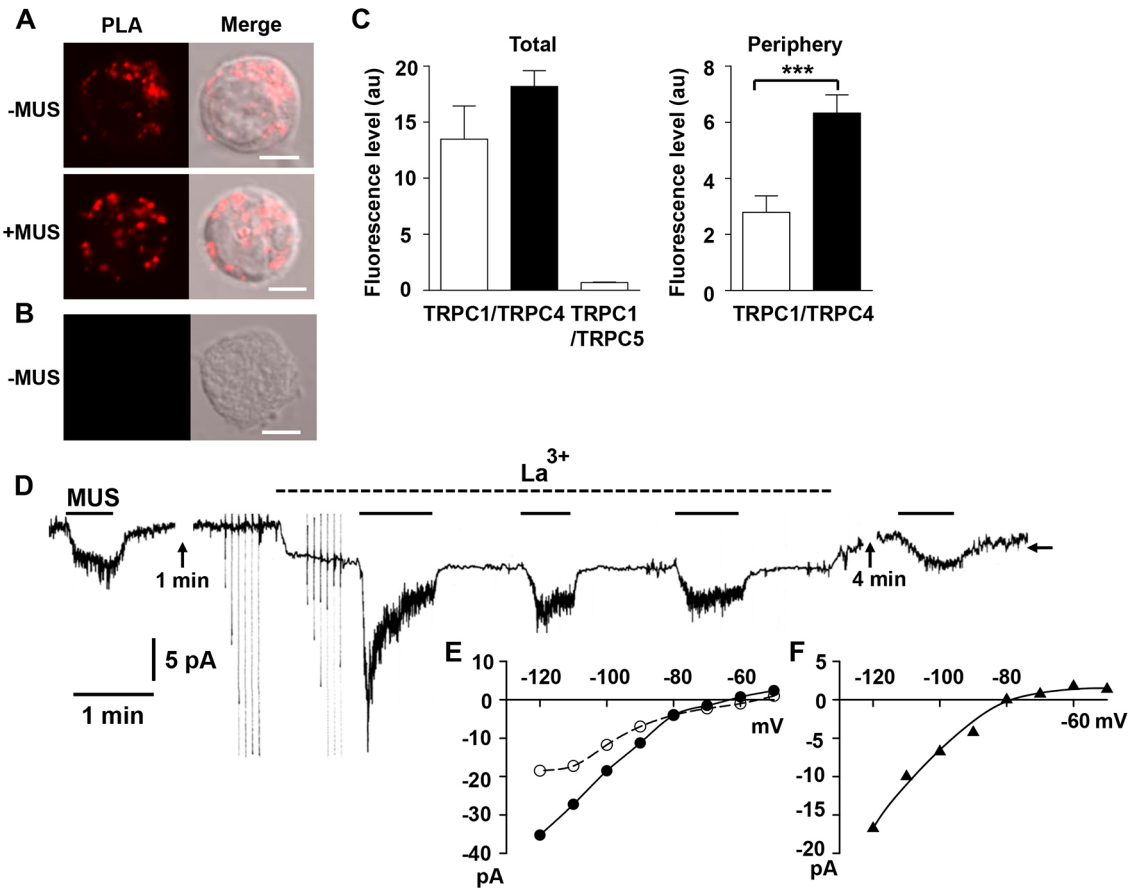

Fig. 8. PLA and electrophysiological analysis for muscarinic trafficking of heteromeric TRPC1–TRPC4 channels in guinea pig AM cells. (A) Translocation of heteromeric TRPC1–TRPC4 channels to the cell periphery in response to muscarine stimulation. The left column represent confocal images of PLA reaction between TRPC1 and TRPC4 and the right column represents a merge of DIC and fluorescence images. Guinea pig AM cells were unstimulated (−MUS) or stimulated with 30 µM muscarine for 2 min (+MUS), then fixed with PFA. PLA was performed with a combination of mouse anti-TRPC1 and rabbit anti-TRPC4 antibodies. (B) PLA for heteromeric channel formation of TRPC1 with TRPC5. Guinea pig AM cells were left unstimulated (−MUS) for 2 min, then fixed with PFA. After fixation, the cells were treated with a combination of rabbit anti-TRPC1 and mouse anti-TRPC5 antibodies. (C) Summary of the levels of PLA products in the whole cell area (Total) and at the cell periphery (Periphery). The data represent means±s.e.m. of n=10 (open: −MUS) and n=14 (closed: +MUS) for TRPC1/TRPC4, and n=9 (open) for TRPC1/TRPC5. ***P<0.001, evaluated by unpaired Student's t-test. (D) Recording traces of whole-cell current in an isolated guinea pig AM cell. The membrane potential was held at −60 mV using the perforated patch clamp method. 10 µM muscarine (MUS) and 600 µM La^{3+} were bath applied during the indicated periods (solid lines for muscarine and interrupted line for La^{3+}). The vertical lines represent currents in response to 50 ms square pulses applied in 10 mV steps every 5 s. The traces were interrupted for indicated times. (E) Current–voltage (I–V) curves in the absence (●) and presence (○) of La^{3+}. Current levels at the end of pulses were measured and plotted against the membrane potentials. (F) I–V curve for La^{3+}-sensitive currents. The La^{3+}-sensitive currents were obtained with subtraction of the current levels in the presence of La^{3+} from those in its absence. Scale bars: 5 µm.

trafficking results in the insertion of heteromeric channels into the cell membrane with consequent depolarization. Indeed, the experiment with extracellularly tagged TRPC channels clearly demonstrated the insertion of TRPC1–TRPC4 heteromeric channels into the cell membrane in response to muscarinic receptor stimulation. TRPC1 channels in the cytoplasm have been shown to be recruited to the cell membrane in response to Ca^{2+} store depletion in HEK293T cells (Alicia et al., 2008) and HSG cells, a cell line originating from a human salivary gland (Cheng et al., 2011), and TRPC1–TRPC4 heteromeric channels function as a store-operated Ca^{2+} entry channel in endothelial cells (Sundivakkam et al., 2012). Although it is possible that muscarinic receptor stimulation recruits TRPC1–TRPC4 channels to the cell membrane as a result of Ca^{2+} store depletion (Sundivakkam et al., 2012), this is unlikely as exposure to caffeine has previously been shown not to result in the development of an inward current in guinea pig AM cells (Inoue and Imanaga, 1998). What is more important is that expression of the constitutively active STIM1 mutant, STIM1D76A, did not result in membrane insertion of TRPC1–TRPC4 channels in PC12 cells under resting conditions, but facilitated insertion of the channel into the cell membrane in response to muscarinic receptor stimulation. When STIM1D76A was expressed in HEK293 cells, the ER became tubular and endoplasmic reticulum–plasma membrane (ER–PM) contacts were greatly expanded (Grigoriev et al., 2008). Although this expansion has been thought to result in the insertion of TRPC1 channels into the cell membrane (Alicia et al., 2008), TRPC1–TRPC4 heteromeric channels in PC12 cells were not inserted into the cell membrane. What allows for this difference between TRPC1 in HEK293 cells and TRPC1–TRPC4 in PC12 cells remains to be explored. At this stage, it would be rational to conclude that ER Ca^{2+} depletion itself does not result in the membrane insertion of TRPC1–TRPC4 channels, but leads to their translocation to the vicinity of the cell membrane, probably as a result of the expansion of ER–PM contacts. This juxtaposition of TRPC1–TRPC4 and the cell membrane may allow for facilitation of membrane insertion in response to muscarinic receptor

Journal of Cell Science (2019) 132, jcs227389. doi:10.1242/jcs.227389

stimulation. Based on current concepts in cell biology, the ER membrane is not thought to directly fuse with the plasma membrane (Saheki and De Camilli, 2017). Thus, the putative mechanism for channel insertion would be exocytotic fusion of vesicles budded off from the ER. This notion may be consistent with the finding that muscarinic receptor stimulation is mandatory for the membrane insertion of TRPC1–TRPC4 in PC12 cells and probably guinea pig AM cells.

The TRPC4 channel, when exogenously expressed in COS-7 cells, has been reported to be trafficked to the cell membrane upon epidermal growth factor (EGF) stimulation, and this EGF-induced membrane insertion was proposed to be mediated by phosphorylation of tyrosine residues near the C-terminus of TRPC4 and the consequent facilitation of Na^+/H^+ exchange regulatory cofactor (NHERF, also known as SLC9A3R1) binding (Odell et al., 2005). We have recently reported that in rat AM cells and PC12 cells, muscarinic M_1 receptor stimulation rapidly induces endocytosis of TASK1 channels through a signal pathway comprising phospholipase C, protein kinase C and Src (Matsuoka and Inoue, 2017). Thus, it is possible that the muscarine-induced trafficking of TRPC1–TRPC4 heteromeric channels is mediated by a similar signaling pathway. However, efficacy and potency of muscarinic agonists to inhibit TASK channels differed from those that induce the trafficking of TRPC1–TRPC4 to the cell periphery (Inoue et al., 2019a). These pharmacological findings are difficult to reconcile with the involvement of a similar signaling pathway. Further studies will be needed to elucidate the molecular mechanism for muscarinic receptor-mediated trafficking of TRPC1–TRPC4 channels.

Roles of STIM1

The roles of STIM1 in GPCR-mediated activation of TRPC channels are complicated and seem to depend on the expression levels of TRPC channels. For example, when TRPC3 proteins are highly expressed, STIM1 is not obligatory for GPCR-mediated activation; however, STIM1 is obligatory in the case of low expression of TRPC3 (Yuan et al., 2007). The present study clearly demonstrated that the simultaneous expression of exogenous STIM1 enhances heteromer formation of TRPC1 and TRPC4. The heteromer formation in PC12 cells expressing no exogenous STIM1 might be ascribed to the presence of endogenous STIM1 (Wang et al., 2015). The intriguing findings here are that heteromer formation was not facilitated by expression of either STIM1ΔCt or STIM1CT mutants, and fully developed with the expression of STIM1_1-448, which contains a CAD region. Furthermore, CAD acted as a dominant negative for STIM1-dependent heteromeric channel formation. Basic residues in CAD (amino acids 342–448) have been shown to bind to acidic residues in the vicinity of the C-terminal end of Orai1 (Park et al., 2009; Lewis, 2011), whereas an extended region (amino acids 251–535) including CAD is also known to bind to TRPC1, TRPC4 or TRPC5 (Yuan et al., 2007; Lee et al., 2010). The sequence near the C-terminus of such TRPC channels is also rich in acidic residues, as is noted with that of Orai1. Thus, it is likely that basic residues in CAD also bind to acidic residues clustered near the C-terminus of TRPC1 or TRPC4. The fact that STIM1CT, comprising the cytoplasmic segment of STIM1, did not facilitate heteromer formation suggests that STIM1 may facilitate heteromer formation of TRPC1 with TRPC4 in the ER. It was recently shown that a coiled-coil domain in the N-terminus and a segment of 20 amino acids in the C-terminus of each of TRPC1 and TRPC4 are prerequisites for heteromer formation (Myeong et al., 2016). Thus, TRPC1 and TRPC4 may be accumulated in the ER through each binding to STIM1, which is known to multimerize, where they then interact to form heteromeric channels. Another interesting finding with STIM1 mutants is that muscarine stimulation failed to induce the trafficking of heteromeric channels in PC12 cells expressing STIM1_1-448. This mutant lacks a motif (TRIP) for binding to end-binding protein 1 (EB1, also known as MAPRE1), which plays an important role in the targeting to microtubule ends of microtubule plus-end tracking proteins, such as STIM1 (Honnappa et al., 2009). Muscarinic receptor stimulation might extend the ER toward the cell membrane through the interaction between STIM1 and EB1 (Várnai et al., 2008) and then facilitate budding from the ER with the consequent fusion of vesicles to the cell membrane. The present results pave the way to exploring how muscarinic receptor stimulation activates TRPC1–TRPC4 heteromeric channels.

In conclusion, the present study demonstrated two obligatory roles of STIM1 for muscarinic activation of TRPC1–TRPC4 channels in PC12 cells: one is to facilitate heteromeric channel formation of TRPC1 with TRPC4, but not TRPC5, in PC12 cells and guinea pig AM cells; the second is to facilitate the insertion of TRPC1–TRPC4 channels into the cell membrane in response to muscarinic receptor stimulation.

MATERIALS AND METHODS

Male Hartley 1-to-2-month-old guinea pigs (*Cavia porcellus*) were used. All procedures for the care and treatment of animals were carried out according to the Japanese Act on the Welfare and Management of Animals and the Guidelines for the Proper Conduct of Animal Experiments issued by the Science Council of Japan. The experimental protocols were approved by the Institutional Animal Care and Use Committee of the University of Occupational and Environmental Health (AE07-012). All efforts were made to minimize suffering and to reduce the number of animals used in this study.

Immunocytochemistry

Immunocytochemical staining in an acutely isolated AM cell was performed as described elsewhere (Inoue et al., 2000). Briefly, the animals were killed by cervical dislocation, and adrenal glands were excised and immediately put into ice-cold Ca^{2+}-deficient saline in which 1.8 mM $CaCl_2$ was omitted from standard saline. The standard saline contained 137 mM NaCl, 5.4 mM KCl, 1.8 mM $CaCl_2$, 0.5 mM $MgCl_2$, 0.53 mM NaH_2PO_4, 5 mM D-glucose, and 4 mM NaOH (pH 7.4). Microscissors and forceps were used to remove the adrenal cortex from the adrenal medulla under stereoscopic observations. The adrenal medulla was cut into half and then treated with 10 mg of collagenase (Yakult Pharmaceutical Industry, Kunitachi, Japan) dissolved in 1.5 ml of Ca^{2+}-deficient saline for 15 min while the preparations were gently stirred with bubbles of O_2 gas. This procedure of digestion was repeated twice with a fresh enzyme solution. After enzymatic digestion, one or two pieces of adrenal medullae in Ca^{2+}-deficient saline were placed on a glass-bottomed dish (Matek, Ashland, MA, USA) and then dissociated using fine needles under microscopic observations. The resulting isolated AM cells were left for 30 min to settle on the glass bottom before muscarine stimulation, and then the cells were fixed in 4% paraformaldehyde (PFA) for 1 h, unless otherwise noted. The fixed cells were incubated in phosphate-buffered saline (PBS) with 5% fetal bovine serum and 0.3% Triton X-100 for 30 min. For indirect immunofluorescence studies, cells were treated overnight with primary antibodies (see 'Reagent details' below). After incubation, the cells were washed three times in PBS and then treated with secondary antibodies conjugated with Alexa Fluor 488, 546 or 633 (1:200; Molecular Probes Thermo Fisher Scientific, Tokyo, Japan). The immunostaining was observed with a confocal laser scanning microscope (LSM5Pascal, Carl Zeiss, Tokyo, Japan). Excitation wavelength and emission filters were a 458 nm laser and 475–525 nm filter for cyan fluorescent protein (CFP) (CFP-like fluorescence), a 488 nm laser and 510–560 nm filter for Alexa

488 and green fluorescent protein (GFP) (FITC-like fluorescence), 543 nm laser and 560 nm long pass filter for Alexa 546 (rhodamine-like fluorescence), and a 633 nm laser and 650 nm long pass filter for Alexa 633 (Alexa 633-like fluorescence), respectively. Experiments were carried out at 26±2°C.

Voltage-clamp recording

The perforated patch clamp method was used to record the whole-cell current in isolated guinea pig AM cells, as described elsewhere (Inoue et al., 2008). Briefly, digested adrenal medullae in Ca^{2+}-deficient saline were placed in a bath apparatus on the stage of an inverted microscope, and AM cells were dissociated mechanically with fine needles and left for 30 min to settle on the glass bottom before the start of perfusion with the standard saline. The pipette solution contained 120 mM potassium isethionate, 20 mM KCl, 10 mM NaCl, 10 mM HEPES and 2.6 mM KOH (pH 7.2). On the day of the experiment, nystatin dissolved in dimethyl sulfoxide (5 mg in 10 µl) was added to the pipette solution at a final concentration of 100 µg ml^{-1}. The membrane potential was corrected for a liquid junction potential of −3 mV between the pipette solution and standard saline. The current was recorded with an Axopath 200A amplifier (Axon, Foster City, CA, USA) and then fed into a thermal recorder after low-pass filtering at 15 Hz and into a data recorder. To study the I–V curve, 50 ms square pulses were applied in steps of 10 mV from a holding potential of −60 mV, and the current level at the end of pulses was measured and plotted against the membrane potential. The effects of La^{3+} were examined in a saline in which NaH_2PO_4 was omitted from the standard saline.

Plasmid construction

For the examination of membrane insertion of TRPC channels by muscarinic stimulation, FLAG and hemagglutinin (HA) tags were inserted into the first outer loop of TRPC1–GFP (TRPC1–FLAG–GFP) and the third outer loop of TRPC4–GFP (TRPC4–HA–GFP), respectively. Both constructs were created by two-step nucleotide insertion. For TRPC1–FLAG–GFP, the first 12 nucleotides (corresponding to four amino acids, DYKD) of FLAG tag were inserted between Gly359 and Arg360, then the last 12 nucleotides (corresponding to four amino acids, DDDK) were inserted right after the first-inserted nucleotides by PCR-based method. For TRPC4–HA–GFP, the first 15 nucleotides (corresponding to five amino acids, YPYDV) of HA tag were inserted between Cys554 and Glu555, then the last 12 nucleotides (corresponding to four amino acids, PDYA) were inserted right after the first-inserted nucleotides. The following pairs of oligonucleotide primers were utilized: 5′-tttggcgattataaagatagaatcattcacacacct-3′ and 5′-gattctatctttataatcgccaaattgagatttggg-3′ for the first half of FLAG, 5′-aaagatgatgatgactatagaatcattcacacacct-3′ and 5′-gattctatagtcatcatcatctttataatcgccaaa-3′ for the second half of FLAG; 5′-cggtgctatccatatgatgttgagaaacagaacaacgcg-3′ and 5′-tttctcaacatcatatggatagcaccggatgcctttgca-3′ for the first half of HA, 5′-gatgttcctgactaagcggagaaacagaacaacgcg-3′ and 5′-tttctccgcttagtcaggaacatcatatggatagca-3′ for the second half of HA. To create a constitutively active form of STIM1, Asp76 on STIM1–myc was substituted with alanine by a sequential, overlapping, PCR-based method, and the following pair of oligonucleotide primers was utilized: 5′-ctgatg**gcc**gacgatgccaatggtgat-3′ and 5′-atcgtcggccatcagcttatggatgtt-3′.

Cell culture and transfection

Cell culture and transfection were performed as described elsewhere (Matsuoka and Inoue, 2017). Briefly, PC12 cells, provided without authentication by Dr K. Mizuno (Tohoku University, Sendai, Japan), were cultured in Dulbecco's modified Eagle's medium (Invitrogen Life Technologies, Tokyo, Japan) supplemented with 10% fetal bovine serum (Nichirei, Tokyo, Japan) at 37°C in an atmosphere of humidified air (95%) and CO_2 (5%). Lipofectamine 2000 (Invitrogen Life Technologies) was used to transfect PC12 cells with plasmids encoding TRPC1–GFP, TRPC4–GFP, TRPC5–GFP (Shimizu et al., 2006), STIM1–myc (Oh-Hora et al., 2008), YFP–STIM1ΔCT (Covington et al., 2010), mCherry–STIM1_1-448 (Convington et al., 2010), myc–STIM1CT (Huang et al., 2006), and/or CFP–CAD (Park et al., 2009), according to the manufacturer's instructions. The cells were fixed with 4% PFA.

Immunoprecipitation analyses

PC12 cells were seeded in 100-mm dishes and cultured to 70–80% confluence before transfection with plasmids encoding TRPC4–GFP or GFP. The cells were lysed with ice-cold TNE buffer (10 mM Tris-HCl pH 7.4, 1 mM EDTA and 150 mM NaCl), to which 1% Nonidet P-40, 1 mM Na_3VO_4, and a protease inhibitor cocktail (Calbiochem Merk, Tokyo, Japan) were added, and then subjected to centrifugation at 12,000 ***g*** for 30 min at 4°C. The supernatant was collected and used as cell lysate (total cell lysate, TCL). For immunoprecipitation assays, cell lysates were incubated with mouse anti-GFP antibody (1:200; sc-9996; Santa Cruz Biotechnology, Santa Cruz, CA, USA) coupled with protein G-Sepharose (GE Healthcare Bio-Sciences, Tokyo, Japan) at 4°C for 3 h. The beads were washed three times with TNE buffer and then the proteins were eluted with SDS buffer (125 mM Tris-HCl pH 6.8, 2% SDS, 10% glycerol). After addition of 2-mercaptoethanol [final content 5% (vol/vol)] and Bromophenol Blue [0.05% (vol/vol)], the same amount of proteins was fractionated by 10% SDS-polyacrylamide gel electrophoresis and transferred to a polyvinylidene difluoride membrane and then subjected to immunoblot analysis with mouse anti-TRPC1 antibody (1:100; sc-133076; Santa Cruz Biotechnology). The immunoblot was repeated three times.

Proximity ligation assay (PLA)

Fixed PC12 cells expressing exogenous proteins, or AM cells were treated with a combination of mouse and rabbit antibodies. The PLA reaction was detected with the Duolink In Situ kit (Olink Bioscience, Uppsala, Sweden) according to the manufacturer's instructions. The PLA reactions occur between target proteins that are located in close proximity to each other (< 40 nm) (Söderberg et al., 2006). The fluorescent signals were observed as rhodamine-like fluorescence using a confocal laser scanning microscope.

Ca^{2+} measurement

The ratiometric method was used to investigate effects on intracellular Ca^{2+} concentration ($[Ca^{2+}]_i$). PC12 cells were maintained in high-osmolarity saline where 3% sucrose was added to standard saline. The cells were incubated in 5 µM Fura-2 acetoxymethyl ester-containing high osmolarity saline for 1 h and then for 30 min in Fura-2 acetoxymethyl ester-free solution. To measure a change in $[Ca^{2+}]_i$, an inverted microscope (IX70; Olympus, Tokyo, Japan) equipped with a xenon burner light source and power supply (AH2-RX; Olympus) was used under operation by the image acquisition software HCImage (Hamamatsu Photonics KK, Hamamatsu, Japan). Fura-2 was alternatively excited at 340 and 380 nm each for 300 ms and emission at 510 nm was measured, and then the Fura-2 ratio (emission evoked at 340 nm/emission evoked at 380 nm) was calculated. This protocol was applied every 900 ms. To stimulate cells, 100 µl of standard saline containing 300 µM muscarine with or without 100 µM ML204, a specific inhibitor for TRPC4 and TRPC5 (Miller et al., 2011), was added to 900 µl of dish solution ∼1 min after the start of measurement.

Statistics

All statistical analyses were performed with Prism (v6.07; GraphPad, La Jolla, CA, USA) or Sigma Plot (v13.0; Systat Software, San Jose, CA, USA). The data are presented as means±s.e.m. and *n* represents the number of cells examined. When data had been shown to have a normal distribution (Shapiro–Wilk), statistical difference was evaluated with a two-tailed Student's *t*-test or a one-way ANOVA followed by a post hoc test (Tukey's multiple comparison test). Difference was considered significant when $P<0.05$. Statistical significance is indicated as $*P<0.05$, $**P<0.01$ and $***P<0.001$.

Reagent details

Muscarine chloride and ML204 were obtained from Sigma-Aldrich (Tokyo, Japan). Fura-2 acetoxymethyl ester was from Dojindo (Kumamoto, Japan). Mouse (1:200; sc-133076) and rabbit (1:200; sc-20110) anti-TRPC1, mouse anti-myc (1:100; sc-40), mouse anti-FLAG (1:100; sc-166355), mouse anti-HA (1:100; sc-7392), rabbit anti-GFP (1:100; sc-8334) antibodies were from Santa Cruz Biotechnology; mouse anti-Na pump α1 subunit antibody (1:100; 05-369) was from Upstate Biotechnology (Lake Placid, NY,USA); mouse anti-STIM1 antibody (1:100; 610954) was from

BD Transduction Laboratories (San Jose, CA, USA); rabbit anti-HA antibody (1:100; A190-108A) was from Bethyl Laboratories (Montgomery, TX, USA); mouse anti-TRPC4 (1:200; 75-119) and mouse anti-TRPC5 (1:200; 75-104) antibodies were from Antibodies Incorporated (Davis, CA, USA); rabbit anti-TRPC4 antibody (1:200; ACC-018) was from Alomone Labs (Jerusalem, Israel). A plasmid encoding mouse STIM1–myc was created by Dr A. Rao (Harvard University, Cambridge, MA, USA) and purchased from Addgene (88415; Cambridge, MA, USA); plasmids encoding yellow fluorescent protein (YFP)-tagged human STIM1ΔCt, mCherry-tagged human STIM1_1-448, and CFP-tagged CAD were gifts from Dr R. S. Lewis (Stanford University, Stanford, CA, USA); a plasmid encoding myc-tagged human STIM1CT was a gift from Dr P. Worley (Johns Hopkins University, Baltimore, MD, USA); mouse TRPC1α, mouse TRPC1α–GFP, mouse TRPC4β, mouse TRPC4β–GFP, and mouse TRPC5–GFP constructs were gifts from Dr Y. Mori (Kyoto University, Kyoto, Japan).

Acknowledgements
The authors are grateful to Drs R. S. Lewis (Stanford University), P. Worley (Johns Hopkins University), and Y. Mori (Kyoto University) for the generous gifts of cDNA constructs.

Competing interests
The authors declare no competing or financial interests.

Author contributions
Conceptualization: K.H., H.M., M.I.; Methodology: K.H.; Validation: M.I.; Formal analysis: K.H.; Investigation: K.H., H.M., M.I.; Resources: K.H.; Writing - original draft: M.I.; Supervision: M.I.; Funding acquisition: H.M., M.I.

Funding
This study was supported, in part, by the Japan Society for the Promotion of Science Grants-in-Aid for Scientific Research (KAKENHI; 17K0855 to M.I. and 18K06865 to H.M.).

References
Alfonso, S., Benito, O., Alicia, S., Angelica, Z., Patricia, G., Diana, K. and Vaca, L. (2008). Regulation of the cellular localization and function of human transient receptor potential channel 1 by other members of the TRPC family. *Cell Calcium* **43**, 375-387. doi:10.1016/j.ceca.2007.07.004

Alicia, S., Angélica, Z., Carlos, S., Alfonso, S. and Vaca, L. (2008). STIM1 converts TRPC1 from a receptor-operated to a store-operated channel: moving TRPC1 in and out of lipid rafts. *Cell Calcium* **44**, 479-491. doi:10.1016/j.ceca.2008.03.001

Bezzerides, V. J., Ramsey, I. S., Kotecha, S., Greka, A. and Clapham, D. E. (2004). Rapid vesicular translocation and insertion of TRP channels. *Nat. Cell Biol.* **6**, 709-720. doi:10.1038/ncb1150

Cayouette, S., Lussier, M. P., Mathieu, E. L., Bousquet, S. M. and Boulay, G. (2004). Exocytotic insertion of TRPC6 channel into the plasma membrane upon Gq protein-coupled receptor activation. *J. Biol. Chem.* **279**, 7241-7246. doi:10.1074/jbc.M312042200

Cheng, K. T., Liu, X., Ong, H. L., Swaim, W. and Ambudkar, I. S. (2011). Local Ca^{2+} entry via Orai1 regulates plasma membrane recruitment of TRPC1 and controls cytosolic Ca^{2+} signals required for specific cell functions. *PLoS Biol.* **9**, e1001025. doi:10.1371/journal.pbio.1001025

Clapham, D. E. (2003). TRP channels as cellular sensors. *Nature* **426**, 517-524. doi:10.1038/nature02196

Covington, E. D., Wu, M. M. and Lewis, R. S. (2010). Essential role for the CRAC activation domain in store-dependent oligomerization of STIM1. *Mol. Biol. Cell* **21**, 1897-1907. doi:10.1091/mbc.e10-02-0145

DeHaven, W. I., Jones, B. F., Petranka, J. G., Smyth, J. T., Tomita, T., Bird, G. S. and Putney, J. W.Jr (2009). TRPC channels function independently of STIM1 and Orai1. *J. Physiol.* **587**, 2275-2298. doi:10.1113/jphysiol.2009.170431

Ebihara, T., Guo, F., Zhang, L., Kim, J. Y. and Saffen, D. (2006). Muscarinic acetylcholine receptors stimulate Ca^{2+} influx in PC12D cells predominantly via activation of Ca^{2+} store-operated channels. *J. Biochem.* **139**, 449-458. doi:10.1093/jb/mvj064

Goel, M., Sinkins, W. G., Zuo, C. D., Hopfer, U. and Schilling, W. P. (2007). Vasopressin-induced membrane trafficking of TRPC3 and AQP2 channels in cells of the rat renal collecting duct. *Am. J. Physiol. Renal Physiol.* **293**, F1476-F1488. doi:10.1152/ajprenal.00186.2007

Greene, L. A. and Tischler, A. S. (1976). Establishment of a noradrenergic clonal line of rat adrenal pheochromocytoma cells which respond to nerve growth factor. *Proc. Natl. Acad. Sci. USA* **73**, 2424-2428. doi:10.1073/pnas.73.7.2424

Grigoriev, I., Gouveia, S. M., van der Vaart, B., Demmers, J., Smyth, J. T., Honnappa, S., Splinter, D., Steinmetz, M. O., Putney, J. W., Jr, Hoogenraad, C. C. et al. (2008). STIM1 is a MT-plus-end-tracking protein involved in remodeling of the ER. *Curr. Biol.* **18**, 177-182. doi:10.1016/j.cub.2007.12.050

Harada, K., Matsuoka, H., Miyata, H., Matsui, M. and Inoue, M. (2015). Identification of muscarinic receptor subtypes involved in catecholamine secretion in adrenal medullary chromaffin cells by genetic deletion. *Br. J. Pharmacol.* **172**, 1348-1359. doi:10.1111/bph.13011

Honnappa, S., Gouveia, S. M., Weisbrich, A., Damberger, F. F., Bhavesh, N. S., Jawhari, H., Grigoriev, I., van Rijssel, F. J., Buey, R. M., Lawera, A. et al. (2009). An EB1-binding motif acts as a microtubule tip localization signal. *Cell* **138**, 366-376. doi:10.1016/j.cell.2009.04.065

Huang, G. N., Zeng, W., Kim, J. Y., Yuan, J. P., Han, L., Muallem, S. and Worley, P. F. (2006). STIM1 carboxyl-terminus activates native SOC, I(crac) and TRPC1 channels. *Nat. Cell Biol.* **8**, 1003-1010. doi:10.1038/ncb1454

Inoue, M. and Imanaga, I. (1993). G protein-mediated inhibition of inwardly rectifying K^+ channels in guinea pig adrenal chromaffin cells. *Am. J. Physiol.* **265**, C946-C956. doi:10.1152/ajpcell.1993.265.4.C946

Inoue, M. and Imanaga, I. (1998). Activation of Ca^{2+}-dependent K^+ channels by cyanide in guinea pig adrenal chromaffin cells. *Am. J. Physiol.* **274**, C105-C111. doi:10.1152/ajpcell.1998.274.1.C105

Inoue, M. and Kuriyama, H. (1991). Muscarinic receptor is coupled with a cation channel through a GTP-binding protein in guinea pig chromaffin cells. *J. Physiol.* **436**, 511-529. doi:10.1113/jphysiol.1991.sp018564

Inoue, M., Fujishiro, N., Ogawa, K., Muroi, M., Sakamoto, Y., Imanaga, I. and Shioda, S. (2000). Pituitary adenylate cyclase-activating polypeptide may function as a neuromodulator in guinea pig adrenal medulla. *J. Physiol.* **528**, 473-487. doi:10.1111/j.1469-7793.2000.00473.x

Inoue, M., Harada, K., Matsuoka, H., Sata, T. and Warashina, A. (2008). Inhibition of TASK1-like channels by muscarinic receptor stimulation in rat adrenal medullary cells. *J. Neurochem.* **106**, 1804-1814. doi:10.1111/j.1471-4159.2008.05521.x

Inoue, M., Harada, K., Matsuoka, H., Nakamura, J. and Warashina, A. (2012). Mechanisms and roles of muscarinic activation in guinea pig adrenal medullary cells. *Am. J. Physiol. Cell. Physiol.* **303**, C635-C644. doi:10.1152/ajpcell.00147.2012

Inoue, M., Matsuoka, H., Harada, K. and Kao, L. S. (2018). Muscarinic receptors in adrenal chromaffin cells: physiological role and regulation of ion channels. *Pflugers Arch.* **470**, 29-38. doi:10.1007/s00424-017-2047-2

Inoue, M., Harada, K., Matsui, M. and Matsuoka, H. (2019a). Differences among muscarinic agonists in M_1 receptor-mediated nonselective cation channel activation and TASK1 channel inhibition in adrenal medullary cells. *Eur. J. Pharmacol.* **843**, 104-112. doi:10.1016/j.ejphar.2018.11.021

Inoue, M., Matsuoka, H., Lesage, F. and Harada, K. (2019b). Lack of p11 expression facilitates acidity-sensing function of TASK1 channels in mouse adrenal medullary cells. *FASEB J.* **33**, 455-468. doi:10.1096/fj.201800407RR

Jung, S., Muhle, A., Schaefer, M., Strotmann, R., Schultz, G. and Plant, T. D. (2003). Lanthanides potentiate TRPC5 currents by an action at extracellular sites close to the pore mouth. *J. Biol. Chem.* **278**, 3562-3571. doi:10.1074/jbc.M211484200

Kim, J. Y. and Saffen, D. (2005). Activation of M1 muscarinic acetylcholine receptors stimulates the formation of a multiprotein complex centered on TRPC6 channels. *J. Biol. Chem.* **280**, 32035-32047. doi:10.1074/jbc.M500429200

Kim, J., Kwak, M., Jeon, J. P., Myeong, J., Wie, J., Hong, C., Kim, S. Y., Jeon, J. H., Kim, H. J. and So, I. (2014). Isoform- and receptor-specific channel property of canonical transient receptor potential (TRPC)1/4 channels. *Pflugers Arch.* **466**, 491-504. doi:10.1007/s00424-013-1332-y

Lee, K. P., Yuan, J. P., So, I., Worley, P. F. and Muallem, S. (2010). STIM1-dependent and STIM1-independent function of transient receptor potential canonical (TRPC) channels tunes their store-operated mode. *J. Biol. Chem.* **285**, 38666-38673. doi:10.1074/jbc.M110.155036

Lewis, R. S. (2011). Store-operated calcium channels: New perspectives on mechanism and function. *Cold Spring Harb Perspect. Biol.* **3**, a003970. doi:10.1101/cshperspect.a003970

Liou, J., Kim, M. L., Heo, W. D., Jones, J. T., Myers, J. W., Ferrell, J. E., Jr and Meyer, T. (2005). STIM is a Ca^{2+} sensor essential for Ca^{2+}-store-depletion-triggered Ca^{2+} influx. *Curr. Biol.* **15**, 1235-1241. doi:10.1016/j.cub.2005.05.055

Matsuoka, H. and Inoue, M. (2017). Molecular mechanism for muscarinic M_1 receptor-mediated endocytosis of TWIK-related acid-sensitive K^+ 1 channels in rat adrenal medullary cells. *J. Physiol.* **595**, 6851-6867. doi:10.1113/JP275039

Matsuoka, H., Harada, K., Ikeda, T., Uetsuki, K., Sata, T., Warashina, A. and Inoue, M. (2009). Ca^{2+} pathway involved in the refilling of store sites in rat adrenal medullary cells. *Am. J. Physiol. Cell. Physiol.* **296**, C889-C899. doi:10.1152/ajpcell.00439.2008

Miller, M., Shi, J., Zhu, Y., Kustov, M., Tian, J.-B., Stevens, A., Wu, M., Xu, J., Long, S., Yang, P. et al. (2011). Identification of ML204, novel potent antagonist that selectively modulates native TRPC4/C5 ion channels. *J. Biol. Chem.* **286**, 33436-33446. doi:10.1074/jbc.M111.274167

Myeong, J., Ko, J., Hong, C., Yang, D., Lee, K. P., Jeon, J. H. and So, I. (2016). The interaction domains of transient receptor potential canonical (TRPC)1/4 and

TRPC1/5 heteromultimeric channels. *Biochem. Biophys. Res. Commun.* **474**, 476-481. doi:10.1016/j.bbrc.2016.04.138

Odell, A. F., Scott, J. L. and Van Helden, D. F. (2005). Epidermal growth factor induces tyrosine phosphorylation, membrane insertion, and activation of transient receptor potential channel 4. *J. Biol. Chem.* **280**, 37974-37987. doi:10.1074/jbc.M503646200

Oh-Hora, M., Yamashita, M., Hogan, P. G., Sharma, S., Lamperti, E., Chung, W., Prakriya, M., Feske, S. and Rao, A. (2008). Dual functions for the endoplasmic reticulum calcium sensors STIM1 and STIM2 in T cell activation and tolerance. *Nat. Immunol.* **9**, 432-443. doi:10.1038/ni1574

Olivos, L. and Artalejo, A. R. (2008). Muscarinic excitation-secretion coupling in chromaffin cells. *Acta Physiol. (Oxf)* **192**, 213-220. doi:10.1111/j.1748-1716.2007.01816.x

Park, C. Y., Hoover, P. J., Mullins, F. M., Bachhawat, P., Covington, E. D., Raunser, S., Walz, T., Garcia, K. C., Dolmetsch, R. E. and Lewis, R. S. (2009). STIM1 clusters and activates CRAC channels via direct binding of a cytosolic domain to Orai1. *Cell* **136**, 876-890. doi:10.1016/j.cell.2009.02.014

Saheki, Y. and De Camilli, P. (2017). Endoplasmic reticulum-plasma membrane contact sites. *Annu. Rev. Biochem.* **86**, 659-684. doi:10.1146/annurev-biochem-061516-044932

Schaefer, M., Plant, T. D., Obukhov, A. G., Hofmann, T., Gudermann, T. and Schultz, G. (2000). Receptor-mediated regulation of the nonselective cation channels TRPC4 and TRPC5. *J. Biol. Chem.* **275**, 17517-17526. doi:10.1074/jbc.275.23.17517

Semtner, M., Schaefer, M., Pinkenburg, O. and Plant, T. D. (2007). Potentiation of TRPC5 by protons. *J. Biol. Chem.* **282**, 33868-33878. doi:10.1074/jbc.M702577200

Shimizu, S., Yoshida, T., Wakamori, M., Ishii, M., Okada, T., Takahashi, M., Seto, M., Sakurada, K., Kiuchi, Y. and Mori, Y. (2006). Ca^{2+}-calmodulin-dependent myosin light chain kinase is essential for activation of TRPC5 channels expressed in HEK293 cells. *J. Physiol.* **570**, 219-235. doi:10.1113/jphysiol.2005.097998

Soboloff, J., Rothberg, B. S., Madesh, M. and Gill, D. L. (2012). STIM proteins: Dynamic calcium signal transducers. *Nat. Rev. Mol. Cell Biol.* **13**, 549-565. doi:10.1038/nrm3414

Söderberg, O., Gullberg, M., Jarvius, M., Ridderstrale, K., Leuchowius, K. J., Jarvius, J., Wester, K., Hydbring, P., Bahram, F., Larsson, L. G. et al. (2006). Direct observation of individual endogenous protein complexes in situ by proximity ligation. *Nat. Methods* **3**, 995-1000. doi:10.1038/nmeth947

Strübing, C., Krapivinsky, G., Krapivinsky, L. and Clapham, D. E. (2001). TRPC1 and TRPC5 form a novel cation channel in mammalian brain. *Neuron* **29**, 645-655. doi:10.1016/S0896-6273(01)00240-9

Sundivakkam, P. C., Freichel, M., Singh, V., Yuan, J. P., Vogel, S. M., Flockerzi, V., Malik, A. B. and Tiruppathi, C. (2012). The Ca^{2+} sensor stromal interaction molecule 1 (STIM1) is necessary and sufficient for the store-operated Ca^{2+} entry function of transient receptor potential canonical (TRPC) 1 and 4 channels in endothelial cells. *Mol. Pharmacol.* **81**, 510-526. doi:10.1124/mol.111.074658

Várnai, P., Hunyady, L. and Balla, T. (2009). STIM and orai: The long-awaited constituents of store-operated calcium entry. *Trends Pharmacol. Sci.* **30**, 118-128. doi:10.1016/j.tips.2008.11.005

Wang, X., Liu, J., Jin, N. A., Xu, D., Wang, J., Han, Y. and Yin, N. (2015). Fructus corni extract-induced neuritogenesis in PC12 cells is associated with the suppression of stromal interaction molecule 1 expression and inhibition of Ca^{2+} influx. *Exp. Ther. Med.* **9**, 1773-1779. doi:10.3892/etm.2015.2316

Yuan, J. P., Zeng, W., Huang, G. N., Worley, P. F. and Muallem, S. (2007). STIM1 heteromultimerizes TRPC channels to determine their function as store-operated channels. *Nat. Cell Biol.* **9**, 636-645. doi:10.1038/ncb1590